Synthesis of Novel Dithienothiophene- and 2,7-Carbazole-Based Conjugated Polymers and H-Bonded Effects on Electrochromic and Photovoltaic Properties

Hsiao-Ping Fang,[1] Jia-Wei Lin,[1] I-Hung Chiang,[1] Chih-Wei Chu,[2,3] Kung-Hwa Wei,[1] Hong-Cheu Lin[1]

[1]Department of Materials Science and Engineering, National Chiao Tung University, Hsinchu, Taiwan, Republic of China
[2]Department of Photonics, National Chiao Tung University, Hsinchu, Taiwan, Republic of China
[3]Research Center for Applied Sciences, Academia Sinica, Taipei, Taiwan, Republic of China
Correspondence to: C.-W. Chu (E-mail: gchu@gate.sinica.edu.tw) or H.-C. Lin (E-mail: linhc@mail.nctu.edu.tw)

Received 14 June 2012; accepted 5 August 2012; published online 11 September 2012
DOI: 10.1002/pola.26336

ABSTRACT: Three kinds of dithienothiophene/carbazole-based conjugated polymers (**P1–P3**), which bear acid-protected and benzoic acid pendants in **P2** and **P3**, respectively, were synthesized via Suzuki coupling reaction. Interestingly, **P1–P3** exhibited reversible electrochromism during the oxidation processes of cyclic voltammogram studies, and **P3** (with H-bonds) revealed the best electrochromic property with the most noticeable color change. According to powder X-ray diffraction (XRD) analysis, these polymers exhibited obvious diffraction features indicating bilayered packings between polymer backbones and π-π stacking between layers in the solid state. Compared with the XRD data of **P2** (without H-bands), H-bonds of **P3** induced a higher crystallinity in the small-angle region (corresponding to a higher ordered bilayered packings between polymer backbones), but with a similar crystallinity in the wide angle region indicating a comparable π-π stacking distance between layers. Moreover, based on the preliminary photovoltaic properties of PSC devices (**P1–P3** blended individually with PCBM acceptor in the weight ratio of 1:1), **P3** (with H-bonds) possessed the highest power conversion efficiency of 0.61% (with $J_{sc} = 2.26$ mA/cm^2, FF = 29.8%, and $V_{oc} = 0.9$ V). In contrast to **P2** (without H-bands), the thermal stability, crystallinity, and electrochromic along with photovoltaic properties of **P3** were generally enhanced due to its H-bonded effects. © 2012 Wiley Periodicals, Inc. J Polym Sci Part A: Polym Chem 50: 5011–5022, 2012

KEYWORDS: electrochromism; functionalization of polymers; heterocyclic conjugated polymer; solar cell; supramolecular structures; WAXS

INTRODUCTION Novel materials are developed for organic optoelectronic devices, such as polymeric solar cells (PSCs), which is a popular research topic in recent decades, because they are low cost and green materials for sustainable resources to reduce consumptions of fossil energy and nuclear power.[1] In particularly, bulk heterojunction (BHJ) solar cells consisting of electron-donating conjugated polymers blended with electron-accepting fullerenes are fabricated in solid thin films.[2] Up to now, regio-regular poly[2-methoxy-5-(3′,7′-dimethyloctyloxy)-*p*-phenylenevinylene] (MDMO-PPV)[3] and poly(3-hexylthiophene) (P3HT)[4] as electron donors blended with [6,6]-phenyl-C61-butyric acid methyl ester (PCBM) as an electron acceptor approached high power conversion efficiency (PCE) values of 5.0% in PSCs. More recently, the PCE values of BHJ solar cells using new low-band gap conjugated polymers have reached 6 to 8%.[5,6] The PCE values of BHJ solar cells were affected by, for example, the energy band gaps of polymers, which is related to the chemical structure of the conjugated polymers. In order to improve the thermal stabilities of polymers by longer conjugation lengths and more rigid structures, novel heteroaromatic fused-ring derivatives, including fused dithienothiophene and carbazole units, are integrated into the polymer backbones. Carbazole unit, which is well known to be a good electron-donating moiety[7] due to its fully aromatic structure, can improve chemical stability in contrast to fluorene unit, and thus poly(2,7-carbazole)s are attractive candidates for solar cells.[8] New carbazole-based copolymers utilized in BHJ solar cells were also reported to achieve a PCE value of 4.3%.[9] According to all these results, the development of new polymers based on carbazole units should have interesting features for the photovoltaic applications. Dithieno[3,2-b:2′,3′-d]thiophene (DTT) unit is a sulfur-rich (three S atoms) and electron-rich building block to make the polymer backbones more rigid and coplanar, and thus to have longer π-conjugation and absorption lengths along with narrower band gaps.[10,11(a)] Due to the limiting intramolecular rotation in the fused-ring structures, such as DTT, the π-orbital overlaps in conjugated

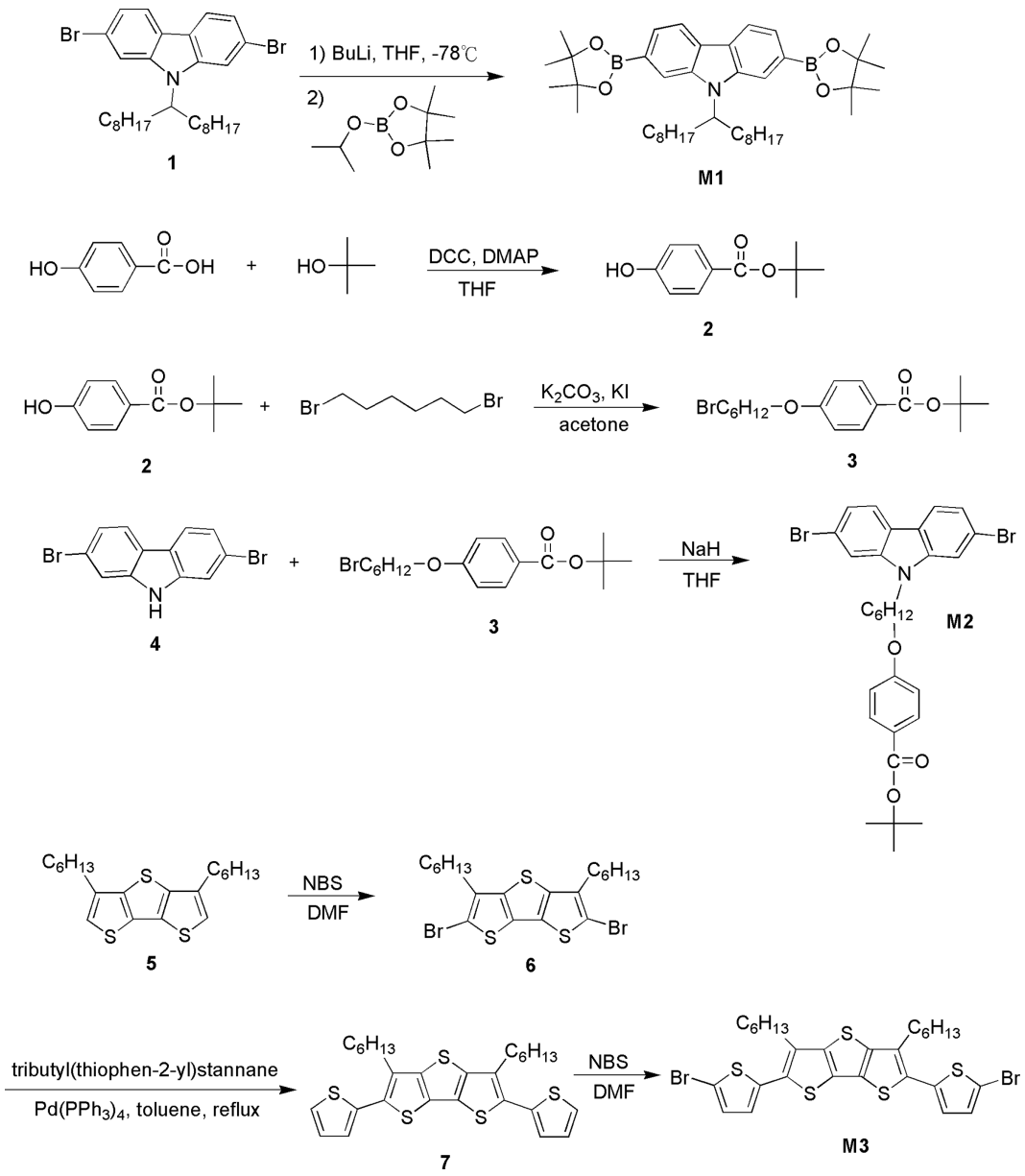

SCHEME 1 Synthetic routes of monomers **M1**–**M3**.

molecules could be maximized to enhance intermolecular charge transports.[11(b,c)] In order to improve the solubility of poly(DTT), alkyl-substituted pendants were incorporated into the polymer backbones, which can be applied to organic solar cells[12-15] and field effect transistors (FETs).[15(b)] Hydrogen bonds (H-bonds) are ideal noncovalent interactions to form self-assembled architectures due to their selectivity and directionality. A numerous advantages of H-bonded polymers, such as stronger light absorptions, lower HOMO levels, higher Voc values, higher hole mobilities, and higher crystallinities, were utilized for organic solar cells.[16] Therefore, great efforts have been taken toward the preparation and characterization of photo- and electroactive noncovalent assemblies based on hydrogen bonds (H-bonds). Würthner,[16(a,b)] El-ghayoury et al., and Jonkheijm et al.[16(c,d)] reported H-bonded assemblies of perylene bisimide and melamine derivatives. In addition, El-ghayoury et al. reported a PCE value of 0.39% for PSCs by utilizing a H-bonded polymer containing oligo(*p*-phenylene vinyene) and ureido-pyrimidinone units.[16(c)]Because of several advantages in polymers, including low cost, easy processing, and tunable chemical properties, the conjugated polymers consisting of different heteroaromatic rings, such as thiophene and carbazole, exhibit an electrochromic behavior as well as photovoltaic properties. Based on this concept, two different moieties, i.e., carbazole (**M1** and **M2**) and fused dithienothiophene (**M3**), were applied into electron-donor monomers to synthesize fused-dithienothiophene-based polymers **P1**–**P3**, where **P1** is a model polymer and the acid pendants of **P3** are protected in **P2** to compare the

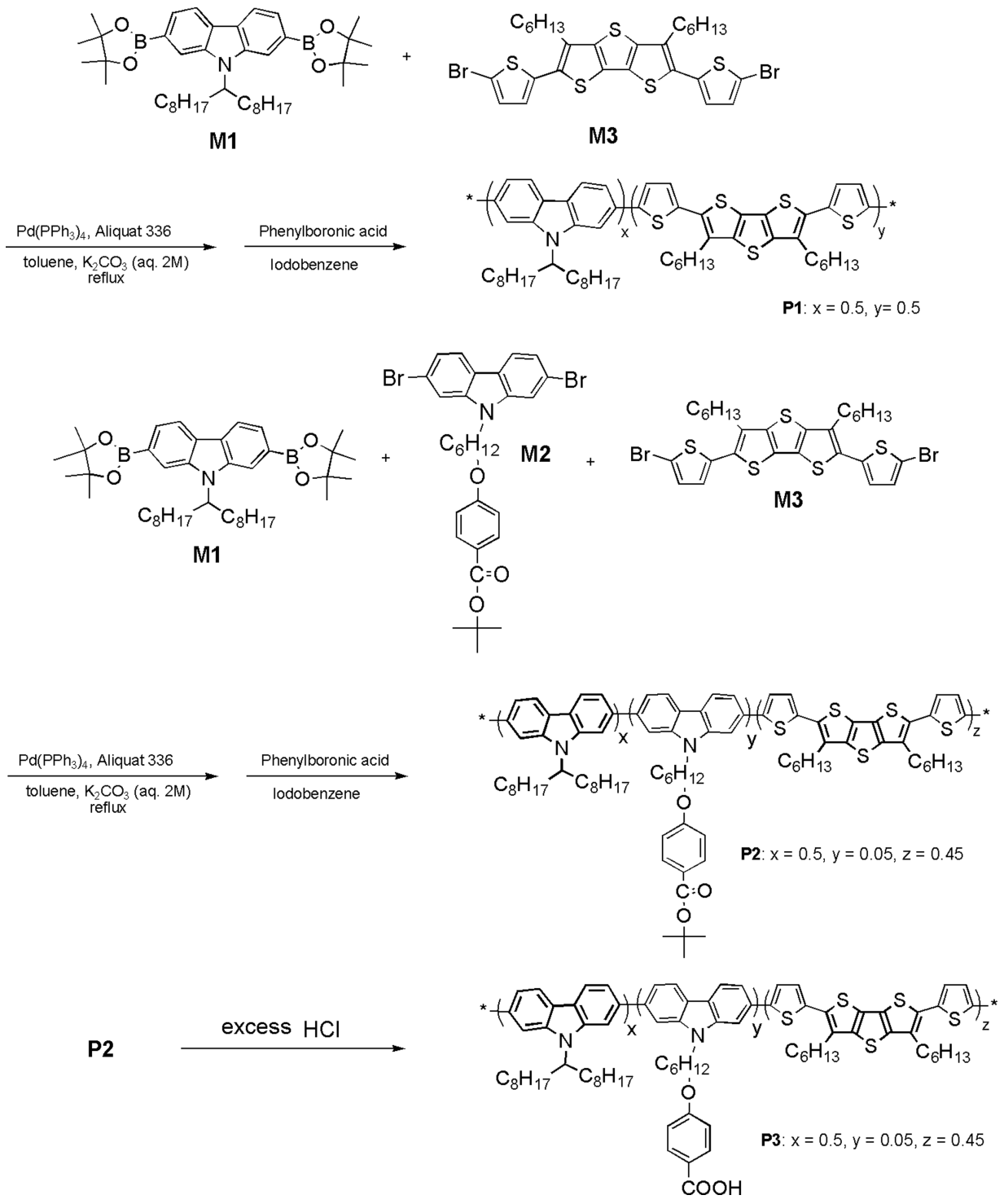

SCHEME 2 Synthetic routes of polymers **P1**–**P3**.

H-bonded effects on their electrochromic behavior as well as photovoltaic properties.

EXPERIMENTAL

Materials

All chemicals and solvents were used as received; 2,7-dibromo-9-(heptadecan-9-yl)-9H-carbazole (**1**),[7] 2,7-dibromocarbazole (**4**),[7] and 3,5-didecanyldithieno[3,2-b:2'3'-d] thiophene) (**5**)[17] were synthesized according to the literature procedures. The synthetic routes of monomers **1**–**3** and polymers **P1**–**P3** are shown in Schemes 1 and 2, and the synthetic procedures of their intermediates were described. Chemicals and solvents were reagent grades and purchased from Aldrich, ACROS, TCI, and Lancaster Chemical Co.

Toluene, tetrahydrofuran, and diethyl ether were distilled to keep anhydrous before use.

Measurements

^{1}H NMR spectra were recorded on a Varian Unity 300 MHz spectrometer using $CDCl_3$ solvents. Elemental analyses were performed on a HERAEUS CHN-OS RAPID elemental analyzer. Transition temperatures were determined by differential scanning calorimetry (DSC, Perkin-Elmer Pyris 7) with a heating and cooling rate of 10 °C/min. Thermogravimetric analyses (TGA) were conducted with a TA instrument Q500 at a heating rate of 10 °C/min under nitrogen. Gel permeation chromatography (GPC) analyses were conducted on a Waters 1515 separation module using polystyrene as a standard and tetrahydrofuran (THF) as an eluent. UV-Vis absorption and photoluminescence (PL) spectra were recorded in dilute THF solutions (10^{-6} M) on a HP G1103A and Hitachi F-4500 spectrophotometer, respectively. Solid films of UV-Vis and PL measurements were spin-coated on a quartz substrate from THF solutions with a concentration of 10 mg/mL. Cyclic voltammetry (CV) measurements were performed using a BAS 100 electrochemical analyzer with a standard three-electrode electrochemical cell in a 0.1 M tetrabutylammonium hexafluorophosphate ($TBAPF_6$) solution (in dimethylformamide, DMF) at room temperature with a scanning rate of 100 mV/s. In each case, a carbon working electrode coated with a thin layer of these polymers, a platinum wire as the counter electrode, and a silver wire as the quasi-reference electrode were used. Ag/AgCl (3 M KCl) electrode was served as a reference electrode for all potentials quoted herein. During the CV measurements, the solutions were purged with nitrogen for 30 s, and the redox couple ferrocene/ferrocenium ion (Fc/Fc^+) was used as an external standard. The corresponding HOMO levels in polymer solutions of **P1–P3** could be calculated from $E_{ox/onset}$ values of the electrochemical experiments (but no reduction curves, i.e., no $E_{red/onset}$ values and LUMO levels, were obtained in the CV measurements). Each onset potential in the CV measurements was defined by the intersection of two tangents drawn at the rising current and background current. The LUMO value of PCBM[18] was in accordance with the literature data. Film thickness and morphology were determined using a Veeco Nanoscope DI 3100 AFM microscope operating in tapping mode. Synchrotron powder X-ray diffraction (XRD) measurements were performed at beamline BL13A of the National Synchrotron Radiation Research Center (NSRRC), Taiwan, where the wavelength of X-ray was 1.026503 Å. The photovoltaic cell (PVC) device structure used in this study was a sandwich configuration of ITO/PEDOT:PSS/active layer/Ca/Al, where the active layer was made of electron donor polymers **P1–P3** mixed with electron acceptor [6,6]-phenyl C_{61} butyric acid methyl ester (PCBM) in a weight ratio1:1. The PVC devices were fabricated according to the procedures similar to those of EL devices. An ITO-coated glass substrate was precleaned and treated with oxygen plasma before use. A thin layer (ca. 50 nm) of PEDOT:PSS was spin-coated on an ITO substrate and heated at 130 °C for 1 h. Subsequently, the preliminary active layer (ca. 100–160 nm) was prepared by spin coating from composite solutions of **P1–P3**: PCBM (w/w = 1:1) in dichlorobenzene (10 mg/mL) by a spin rate of 500 to 800 rpm on the top of the PEDOT:PSS layer. The PVC devices were completed by deposition with a back electrode consisting of Ca (ca. 50 nm) and aluminum (100 nm). The film thicknesses were measured by a profilometer (Dektak3, Veeco/Sloan Instruments Inc.). For PVC measurements, *I–V* curves were recorded under a solar simulator with AM 1.5 irradiation (at 100 mW/cm^2). A 300 W xenon lamp (Oriel, #6258) with AM 1.5 filter (Oriel, #81080 kit) was used as the white light source, and the optical power at the sample was 100 mW/cm^2 detected by Oriel thermopile 71964. The *I–V* characteristics were measured using a CHI 650B potentiostat/galvanostat. The external quantum efficiency (EQE) was measured using a CHI 650B coupled with Oriel Cornerstone 260 monochromator. All PVC devices were prepared and measured under ambient conditions.

Synthesis and Characterization

Materials

9-(Heptadecan-9-yl)-2,7-bis(4,4,5,5-tetramethyl-1,3,2-dioxaborolan-2-yl)-9H-carbazole (M1). To a solution of compound **1** (2,7-dibromo-9-(heptadecan-9-yl)-9*H*-carbazole)[7] (3.62 g, 6.42 mmol) in 150 mL of dry THF, *n*-butyllithium (2.5 M solution in hexane, 5.65 mL, 2.2 eq) was added dropwise, and then stirred to react at −78 °C under nitrogen. After reaction for 2 h at −78 °C, 2-isopropoxy-4,4,5,5-tetramethyl-1,3,2-dioxaborolane (3.15 mL, 2.4 eq) was added carefully to the mixture solution at −78 °C and then the mixture was allowed to warm up to react at room temperature overnight. The final solution was acidified with 100 mL of 10% HCl solution and stirred for 45 min at room temperature and the final solution was extracted with diethyl ether. The organic layer was dried over magnesium sulfate, and the solvent was evaporated. The solvent was removed under reduced pressure, and the residue was purified by recrystallization in methanol/acetone (ca. 10:1) to obtain the final product as a white crystal (2.69 g, yield: 64 %). ^{1}H NMR($CDCl_3$, 300 MHz): δ 8.12 (d, J = 8.0 Hz, 2H), 8.02 (s, 1H), 7.89 (s, 1H), 7.66 (d, J = 8.1 Hz, 2H), 4.73–4.66 (m, 1H), 2.35–2.30 (m, 2H), 1.98–1.90 (m, 2H), 1.39–1.12 (m, 48H), 0.82 (t, J = 7.0 Hz, 6H). MS (FAB): m/z [M^+] 657; calcd. m/z [M^+] 657. Anal. Calcd.: C, 74.89; H, 9.96; N, 2.13. Found: C, 74.42; H, 9.68; N, 2.26.

tert-Butyl 4-hydroxybenzoate (2). Seven grams of 4-hydroxybenzoic acid (50.7 mmol) and 4-dimethylaminopyridine (0.62 g, 0.1 eq) were dissolved in 60 mL of dry THF and stirred in a two-necked flask. Then, 2-methylpropan-2-ol (60 mL, 2-methylpropan-2-ol) and *N*,*N*'-dicyclohexylcarbodiimide (12.6 g, 1.2 eq) were added sequentially. The mixture was purged with nitrogen and vigorously stirred overnight at room temperature. Water was added after reaction, and the reaction mixture was extracted with dichloromethane. Consequently, the organic layer was separated and dried with magnesium sulfate. Solvent was removed under vacuum, and the crude product was purified by chromatography using hexane: ethyl acetate (4:1) as eluent. Subsequently, the pure compound was obtained as a white powder. Yield: 3.95

g (40 %). ^{1}H NMR ($CDCl_3$, 300 MHz): δ 7.87 (d, J = 8.7 Hz, 2H), 6.84 (d, J = 8.5 Hz, 2H), 6.44 (s, 1H), 1.59 (s, 9H).

tert-Butyl 4-(6-bromohexyloxy) benzoate (3). *tert*-Butyl 4-hydroxybenzoate (3.95 g, 20.3 mmol), K_2CO_3 (8.43 g, 3 eq), and KI (0.2 g, 0.06 eq) were dissolved in acetone (150 mL) and stirred in a two-necked flask. The mixture was purged with nitrogen and refluxed overnight. Water was added after reaction, and the reaction mixture was extracted with dichloromethane. Consequently, the organic layer was separated and dried with magnesium sulfate. Solvent was removed under vacuum, and the crude product was purified by chromatography using hexane: ethyl acetate (30:1) as eluent. Subsequently, the pure compound was obtained as a colorless oil. Yield: 6.48 g (89%). ^{1}H NMR($CDCl_3$, 300 MHz): δ 7.89 (d, J = 8.7 Hz, 2H), 6.86 (d, J = 8.5 Hz, 2H), 3.98 (t, J = 6.4 Hz, 2H), 3.40 (t, J = 6.8 Hz, 2H), 1.90–1.77 (m, 4H), 1.56 (s, 9H), 1.51–1.46 (m, 4H).

tert-Butyl 4-(6-(2,7-dibromo-9H-carbazol-9-yl)hexyloxy)-benzoate (M2). NaH (0.36 g, 1.8 eq) and 2,7-dibromo-carbazole[8] (2.71 g, 8.34 mmol) were dissolved in THF (10 mL) and stirred in a two-necked flask and refluxed for 1 h. The solution of *tert*-butyl-4-(6-bromohexyloxy)benzoate (3.7 g, 1.3 eq) in THF (10 mL) was added dropwise and refluxed overnight. Water was added after reaction, and the reaction mixture was extracted with dichloromethane. Consequently, the organic layer was separated and dried with magnesium sulfate. Solvent was removed under vacuum, and the crude product was purified by chromatography using hexane: ethyl acetate (1:7) as eluent. Subsequently, the pure compound was obtained as a colorless oil. Yield: 2.90 g (60 %). ^{1}H NMR($CDCl_3$, 300 MHz): δ 7.90 (m, 4H), 7.53 (d, J = 1.2 Hz, 2H), 7.34 (dd, J = 9.0, 1.6 Hz, 2H), 6.84 (d, J = 8.9 Hz, 2H), 4.22 (t, J = 7.2 Hz, 2H), 3.96 (t, J = 6.29 Hz, 2H), 1.91–1.75 (m, 4H), 1.59–1.44 (m, 13H). MS (EI): m/z [M^+] 601; calcd m/z [M^+] 601. Anal. Calcd.: C, 57.92; H, 5.28; N, 2.33. Found: C, 57.78; H, 5.04; N, 2.52.

2,6-Dibromo-3,5-dihexyldithieno[3,2-b:2'3'-d]thiophene (6). Compound **5** (3,5-dihexyldithieno[3,2-*b*:2'3'-*d*]thiophene)[17] (1.96 g, 5.38 mmol) and NBS (2.39 g, 2.5 eq) were dissolved in 50 mL of DMF. The resulting solution was stirred to react overnight at room temperature under nitrogen. Water (50 mL) was then added, and the organic phase was extracted with ethyl acetate (100 mL) twice, washed with water, and dried with magnesium sulfate. After that, the solvent was removed under reduced pressure to obtain the product. The crude product was purified by column chromatography with hexane to obtain a pale yellow oil (2.51 g). Yield: 89 %. ^{1}H NMR($CDCl_3$, 300 MHz): δ 2.72 (t, J = 7.5 Hz, 4H), 1.75–1.65 (m, 4H), 1.42–1.32 (m, 12H), 0.92–0.88 (m, 6H).

2,6-Dithienyl-3,5-dihexyldithieno[3,2-b:2'3'-d]thiophene (7). Compound **5**, 3,5-dihexyldithieno[3,2-*b*:2'3'-*d*]thiophene (2.46 g, 4.71 mmol), $Pd(PPh_3)_4$ (0.32 g, 0.06 eq), and tributyl(thiophen-2-yl)stannane (3.29 mL, 2.2 eq) were dissolved in toluene (25 mL) and stirred in a two-necked flask to reflux for 12 h. Solvent was removed under vacuum, and the crude product was purified by chromatography using hexane as eluent. Subsequently, the pure compound was obtained as a yellow powder. Yield: 2.12 g (86 %). ^{1}H NMR ($CDCl_3$, 300 MHz): δ 7.35 (dd, J = 5.1, 1.0 Hz, 2H), 7.18 (t, J = 1.0 Hz, 2H), 7.09 (dd, J = 5.1, 3.6 Hz, 2H), 2.91 (t, J = 8.1 Hz, 4H), 1.67–1.61 (m, 4H), 1.42–1.27 (m, 12H), 0.94–0.89 (m, 6H).

2,6-Bis(2'-bromothien-5'-yl) 3,5-dihexyldithieno[3,2-b:2'3'-d] thiophene (M3). About 2.12 g of 2,6-dithienyl-3,5-dihexyldithieno[3,2-*b*:2'3'-*d*]thiophene (4.01 mmol) and NBS (2.1 g, 2.1 eq) were dissolved in DMF (20 mL) and stirred in a flask. The mixture was vigorously stirred overnight at room temperature. Water was added after reaction, and the reaction mixture was extracted with ethyl acetate. Consequently, the organic layer was separated and dried with magnesium sulfate. Solvent was removed under vacuum, and the crude product was purified by chromatography using hexane as eluent. Subsequently, the pure compound was obtained as a pale yellow powder. Yield: 2.0 g (73%). ^{1}H NMR($CDCl_3$, 300 MHz):δ 7.04 (d, J = 3.5 Hz, 2H), 6.9 (d, J = 3.5 Hz, 2H), 2.85 (t, J = 7.3 Hz, 4H), 1.75-1.73 (m, 4H), 1.41–1.26 (m, 12H), 0.92–0.89 (m, 6H). MS (EI): m/z [M^+] 685; calcd. m/z [M^+] 685. Anal. Calcd.: C, 48.98; H, 4.40. Found: C, 48.89; H, 4.63.

General Synthetic Procedures of Polymers P1–P3[19]

The synthetic routes of polymers **P1–P3** are shown in Scheme 2. All of the polymerization procedures were carried out through the palladium (0)-catalyzed Suzuki coupling reactions. In a 25 mL two-necked flask, 0.5 eq of **M1** and **M2** with a molar ratio of **M2**:**M3** = 0:0.5(**P1**) and 0.05:0.45 (**P2**, **P3**) were added into 5 mL of anhydrous toluene. The Pd (0) complex, tetrakis(triphenylphosphine)palladium (1 mol %), was transferred into the mixture under dry environment. Then, 2 M aqueous potassium carbonate and a phase transfer catalyst, that is, Aliquat 336 (several drops), were subsequently transferred to the previous mixture via dropping funnel. The reaction mixture was stirred at 90 °C for 2 days, and then both excess amounts of end-cappers (i.e., iodobenzene and phenylboronic acid) were correspondingly dissolved in 1 mL of anhydrous toluene and reacted for 4 h. The reaction mixture was cooled to 40 °C and added slowly into a vigorously stirred mixture of methanol/water (10:1). The polymers were collected by filtration and reprecipitation from methanol. The crude polymers were further purified by washing with acetone for 3 days in a Soxhlet apparatus to remove oligomers and catalyst residues. The chloroform fractions (350–400 mL) were reduced to 40–50 mL under reduced pressure, and precipitated in acetone along with air-dried overnight finally.

P1

Following the general polymerization procedure, **M1** (0.5 equiv) and **M3** (0.5 equiv) were used in this polymerization to obtain a red powder. Yield: 67%. ^{1}H NMR (ppm, $CDCl_3$): δ 8.06–7.23 (br, 10H), 4.62 (br, 1H), 2.99 (br, 4H), 2.5-0.5 (br). Anal. Calcd.: C, 73.57; H, 7.69; N, 1.51. Found: C, 73.39; H, 7.64; N, 1.35.

P2

Following the general polymerization procedure, **M1** (0.5 equiv), **M2** (0.05 equiv), and **M3** (0.45 equiv) were used in this polymerization to obtain a red powder. Yield: 67%. ^{1}H

TABLE 1 Molecular Weights, Yields, and Thermal Data of Polymers **P1–P3**

Polymer	M_n[a]	M_w[b]	PDI[c]	T_g[d] (°C)	T_d[e] (°C)	Yield (%)
P1	16,600	19,700	1.2	130	421	71.4
P2	19,200	53,100	2.7	138	380	79.5
P3	18,200	50,100	2.7	146	428	70.5

[a] Number average molecular weight.
[b] Weight average molecular weight.
[c] Polydispersity indices (PDI = M_w/M_n).
[d] Glass transition temperature.
[e] Decomposition temperature at 5% weight loss.

NMR (ppm, $CDCl_3$): δ 8.23-7.22 (br, 10H), 4.644 (br, 1H), 3.947 (br, 1H), 3.020 (br, 4H), 2.50–0.66 (br). Anal. Calcd.: C, 75.28; H, 7.49; N, 2.04. Found: C, 75.39; H, 7.44; N, 2.15.

P3

P2 (200 mg) was dissolved in 20 mL toluene, and excess HCl solution was added slowly. The mixture was vigorously stirred for 2 days at 80 °C. The polymers were collected by following the general polymerization procedure to gain a red powder. Yield: 81%. ^{1}H NMR (ppm, $CDCl_3$): δ 8.23–7.22 (br, 10H), 4.654 (br, 1H), 3.950 (br, 1H), 3.025 (br, 4H), 2.50–0.66 (br). Anal. Calcd.: C, 74.84; H, 7.20; N, 2.13. Found: C, 74.79; H, 7.44; N, 2.15.

RESULTS AND DISCUSSION

Syntheses and Chemical Characterization

As outlined in Scheme 1, two monomers **M1** and **M2** based on carbazole moieties were prepared from 2,7-dibromo-9-(heptadecan-9-yl)-9*H*-carbazole (**1**) and 2,7-dibromo-carbazole (**4**) moieties.[7] In addition, **M3** based on dithienothiophene was prepared from 3,5-didecanyldithieno[3,2-b:2′3′-d]thiophene[17] (**5**) using a reduction procedure and followed by dibromination, which were described by Coppo et al.[20] The electron-donating unit of compound **5** was prepared according to the literature procedures. Monomers **M1**–**M3** were satisfactorily characterized by ^{1}H NMR, ^{13}C NMR, MS spectroscopies, and elemental analyses. Polymers **P1–P3** were prepared successfully via Suzuki coupling, where **P1** was produced by **M1** and **M3**; **P2** was synthesized by the copolymerization of monomer **M1** with **M2** and **M3**; and **P3** was prepared by the deprotection of acid in **P2**. The synthetic procedures towards polymers **P1–P3** are outlined in Scheme 2. Most polymers are partly soluble in organic solvents, such as chloroform, THF, and chlorobenzene at room temperature, and completely soluble in high boiling point solvents (e.g., chlorobenzene) at high temperatures. The yields and molecular weights of polymers **P1–P3** determined by gel permeation chromatography (GPC) against polystyrene standards in THF are summarized in Table 1. These results show that considerable molecular weights with high yields (50–81% after Soxhlet extractions) were obtained in these copolymers, where the weight-average molecular weights (M_w) of 19,700 to 53,100 with polydispersity indices (PDI = M_w/M_n) of 1.2 to 2.7 were obtained.

The thermal stabilities and phase transition temperatures of polymers **P1–P3** were characterized by thermogravimetric analyses (TGA) and differential scanning calorimetry (DSC) measurements under nitrogen atmosphere, and the thermal decomposition temperatures (T_d) and glass transition temperatures (T_g) are summarized in Table 1. It is apparent that all polymers exhibited good thermal stabilities, which showed less than 5% weight loss upon heating to 380 to 428 °C. Regarding DSC experiments, samples (weighted 1–5 mg) sealed in an aluminum pan were operated at 30 to 250 °C under N_2 atmosphere with a scan rate of 10 °C/min. These polymers showed glass transition (T_g) temperatures at 130, 138, and 146 °C for **P1**, **P2**, and **P3**, respectively. The T_d and T_g values of **P3** are higher than those of **P2**, which were attributed to the rigid polymer networks of **P3** formed by H-bonds (due to its carboxyl group).

Optical Properties

The optical absorption spectra of polymers **P1–P3** in THF solutions (10^{-6} M) and solid films are shown in Figure 1, and their photophysical properties are demonstrated in Table 2. As can be seen, the absorption spectra of polymers

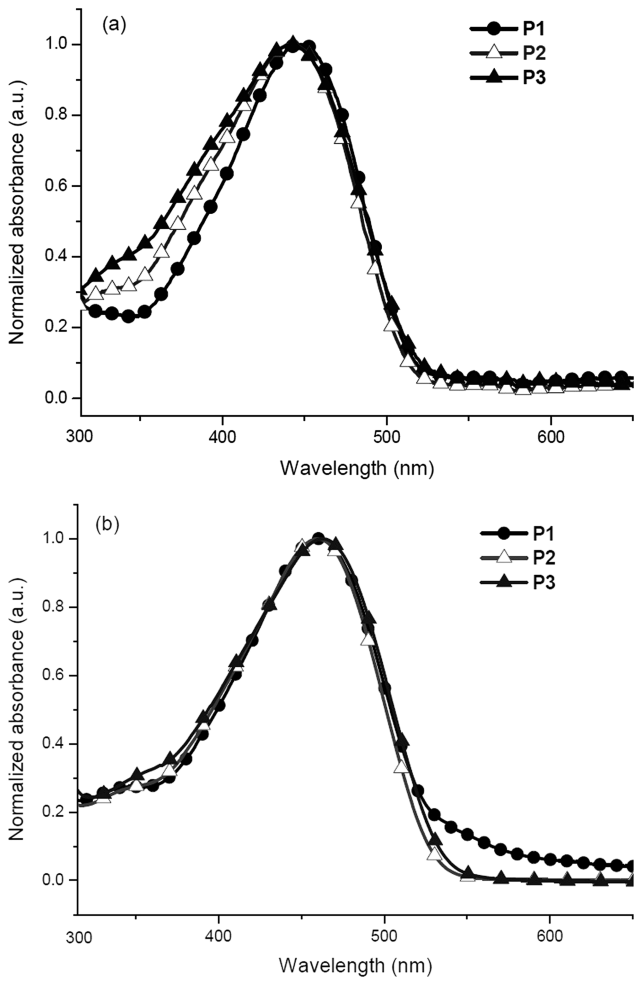

FIGURE 1 Normalized optical absorption spectra of polymers **P1–P3** in (a) solutions (THF) (10^{-6} M) and (b) solid films (spin-coating from THF solutions).

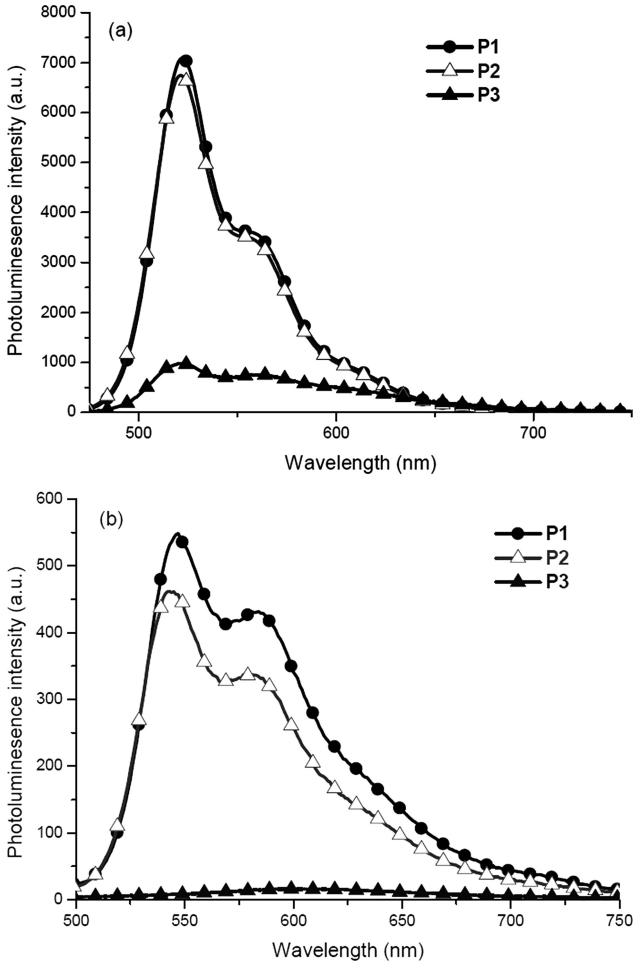

FIGURE 2 Normalized photoluminescence (PL) spectra of polymers **P1-P3** in (a) solutions (THF) (10^{-6} M), and (b) solid films (spin-coating from THF solutions).

P1–P3 covered broad wavelength ranges (300–600 nm) for both solutions and solid films. In addition, **P1–P3** possessed similar maximum absorption wavelengths of 445 and 465 nm in THF solutions and solid films, respectively. Due to the π-π stacking of these polymer chains in solids, the maximum absorption wavelength (465 nm) of **P1–P3** in solid films was red-shifted about 20 nm in contrast to that (445 nm) of their solutions. As shown in Table 2, the optical band gaps (*E*g,opt) of 2.24 to 2.25 eV in polymers **P1–P3** could be determined by the cut-offs of the absorption spectra in solid films.

The PL emission spectra of the polymers in solutions and solid films were illustrated in Figure 2. The photoluminescence (PL) spectra of polymers **P1–P3** in THF solutions and solid films were excited at incident wavelengths of 445 and 465 nm, respectively. Interestingly, in comparison with polymer **P2** in Figure 2, the PL spectra of **P3** containing carboxylic acid moieties were almost quenched in solution and completely quenched in solid film [see Fig. 2(a,b), respectively]. The PL emission of **P3** containing carboxylic acid moieties (COOH) is quenched because its dimeric H-bonded structure is formed to shorten the distance between chromophores and to result in the stacking phenomena to quench the PL emission. In other words, the PL quenching phenomena of H-bonds in **P3** induced by the carboxylic groups might stem from the intersystem crossing from the photo-excited singlet state to the triplet one, where both intramolecular (in solutions) and intermolecular (in solid films) energy transfers along the conjugated backbones might occur. The corresponding optical properties of these polymers in solid films, including the broad and strong optical absorptions, proposed their potential applications in photovoltaic cells described below.

Electrochemical Properties

The electronic states, that is, highest occupied molecular orbital (HOMO) and lowest unoccupied molecular orbital (LUMO) levels, of the polymers were investigated by cyclic voltammetry (CV) measurements in order to understand the charge injection processes in these polymers and their PSC devices. The oxidation cyclic voltammograms of **P1–P3** in solid films and the corresponding electrochromic photos (with a distinct change from orange to black) of **P3** are displayed in Figure 3(a), where the electrochromic activities in **P1** and **P2** were not noticeable to be included due to the lack of H-bonds. The formal potentials and HOMO energy levels (estimated the average oxidation potentials from the electrochemical measurements) are summarized in Table 2. As shown in Figure 3(a), polymers **P1–P3** showed one quasi-reversible oxidation process but no detectable reduction behavior. Therefore, the HOMO energy levels of **P1–P3** can be decided by their quasi-reversible oxidation peaks

TABLE 2 Photophysical Data in THF Solutions and Solid Films, Optical Band Gaps, Electrochemical Potentials, Energy Levels, and Band Gap Energies of Polymers **P1–P3**

Polymer	λ_{abs}, Sol[a] (nm)	λ_{abs}, Film[b] (nm)	λ_{PL}, Film[b] (nm)	$E_{1/2}$[d] (ox)	E_{HOMO} (eV)[e]	E_{LUMO} (eV)[f]	$E_{g,opt}$ (eV)[g]
P1	445	465	546	0.89	−5.58	−3.34	2.24
P2	445	465	543	0.91	−5.60	−3.35	2.25
P3	445	465	–[c]	0.91	−5.60	−3.35	2.25

[a] The absorption spectra were recorded in dilute THF solution at room temperature.
[b] The absorption and PL films were spin-coated from 10 mg/1 mL THF solution.
[c] PL peaks were not detectable due to the PL quenching behavior.
[d] $E_{1/2}$ was the average value of oxidation.
[e] $E_{HOMO} = [-(E_{1/2} - 0.11) - 4.8]$ eV where 0.11 V is the value for ferrocene versus Ag/Ag+ and 4.8 eV is the energy level of ferrocene below the vacuum.
[f] LUMO = HOMO − $E_{g,opt.}$
[g] Optical band gaps were estimated from the absorption spectra in solid films by using the equation of $E_g = 1240/\lambda_{edge}$

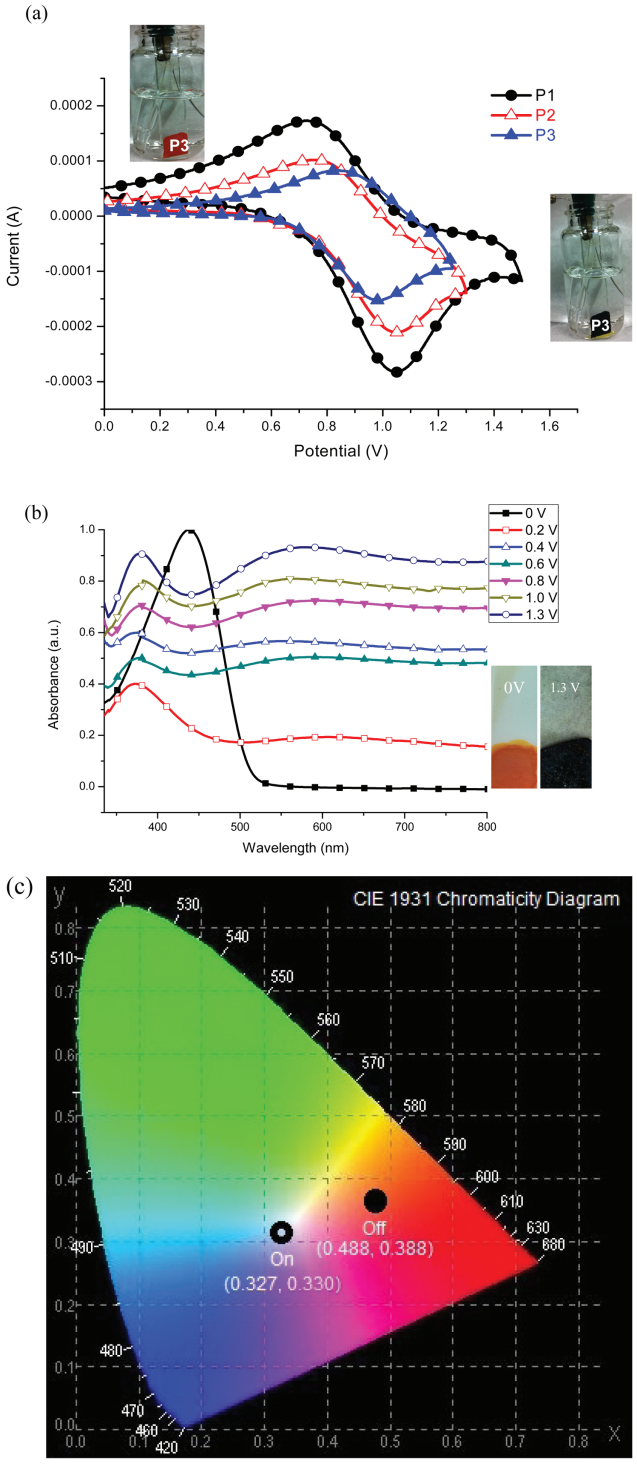

FIGURE 3 (a) Cyclic voltammograms of polymers **P1–P3** (in solid films) at a scan rate of 100 mV/s, (b) absorption spectra and optical images of **P3** on ITO at various applied potentials (0 V–1.3 V), (c) CIE chromaticity diagram of **P3** at "off" (0 V) and "on" (+1.3 V) states.

correspondingly. The moderate onset oxidation potentials of **P1–P3** occurred between 0.6 and 1.2 V from which the estimated HOMO levels of −5.58 to −5.60 eV were acquired according to the following equation:[21,22] $E_{HOMO/LUMO} = [-(E_{onset\ (vs\ Ag/AgCl)} - E_{onset\ (Fc/Fc\ +\ vs\ Ag/AgCl)} - 4.8]$ eV, where 4.8 eV is the energy level of ferrocene below the vacuum level and $E_{onset\ (Fc/Fc\ +\ vs\ Ag/AgCl)} = 0.11$ eV. Due to the lack of their reduction peaks, the LUMO energy levels of **P1–P3** can not be determined, but the LUMO levels can be elucidated by subtracting the optical band gaps (Eg,opt) from the HOMO energy levels of **P1–P3**. The electrochemical reductions of polymers **P1–P3** showed LUMO energy levels at about −3.34 to −3.35 eV, which represent to possess high electron affinities and also make these polymers suitable donors for electron injection and transporting to PCBM acceptor (with 0.4 eV offsets in LUMO levels regarding PCBM with a LUMO level of −3.75 eV,[23] as shown in Fig. 4) for the bulk heterojunction polymer solar cell devices.[24] As the potentials of **P1–P3** were gradually increased to +1.3 to 1.5 V in Figure 3(a), due to the higher stability and crystallinity induced by H-bonds, only the electrochromic color of **P3** changed noticeably from orange (in the neutral state) to black (in the oxidation state) and the color change could be easily detected by naked eye. The absorption spectra (at various applied potentials), and optical feature images along with CIE chromaticity diagram of **P3** film under neutralization (0.0 V) and oxidation (1.3 V) states are demonstrated in Figure 3(b,c), where **P3** illustrated a hypsochromic absorption and an enhanced absorption in the range of 500 to 800 nm during the oxidation process (from 0.0 to 1.3 V). Therefore, **P3** is a good candidate for the electrochromic application due to its distinct color change with easy processibility in different solvents (in DCM, THF, and $CHCl_3$).

X-Ray Diffraction (XRD) Analyses

As shown in Figure 5(a,b), powder X-ray diffraction (XRD) patterns of polymers **P1–P3** were acquired to investigate the molecular organization and morphological change. The measurements were proceeded on drop-cast films prepared from 0.5 wt % solutions in THF after the thermal treatment of about 150 °C for 10 min and were then cooled to room

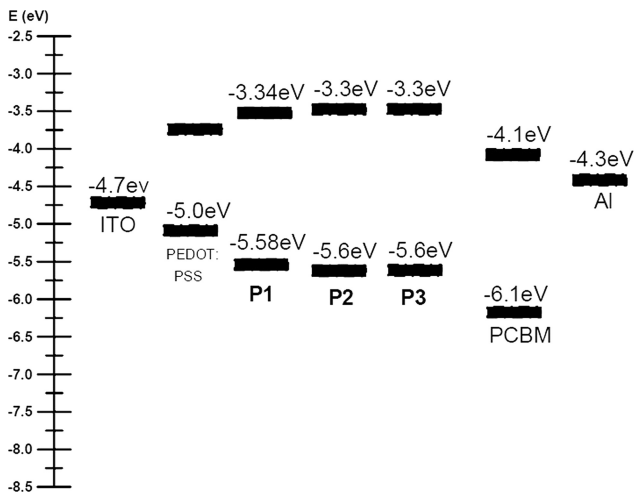

FIGURE 4 Energy band diagrams with HOMO/LUMO levels of donor polymers **P1–P3** in relation to the work functions of ITO and Al.

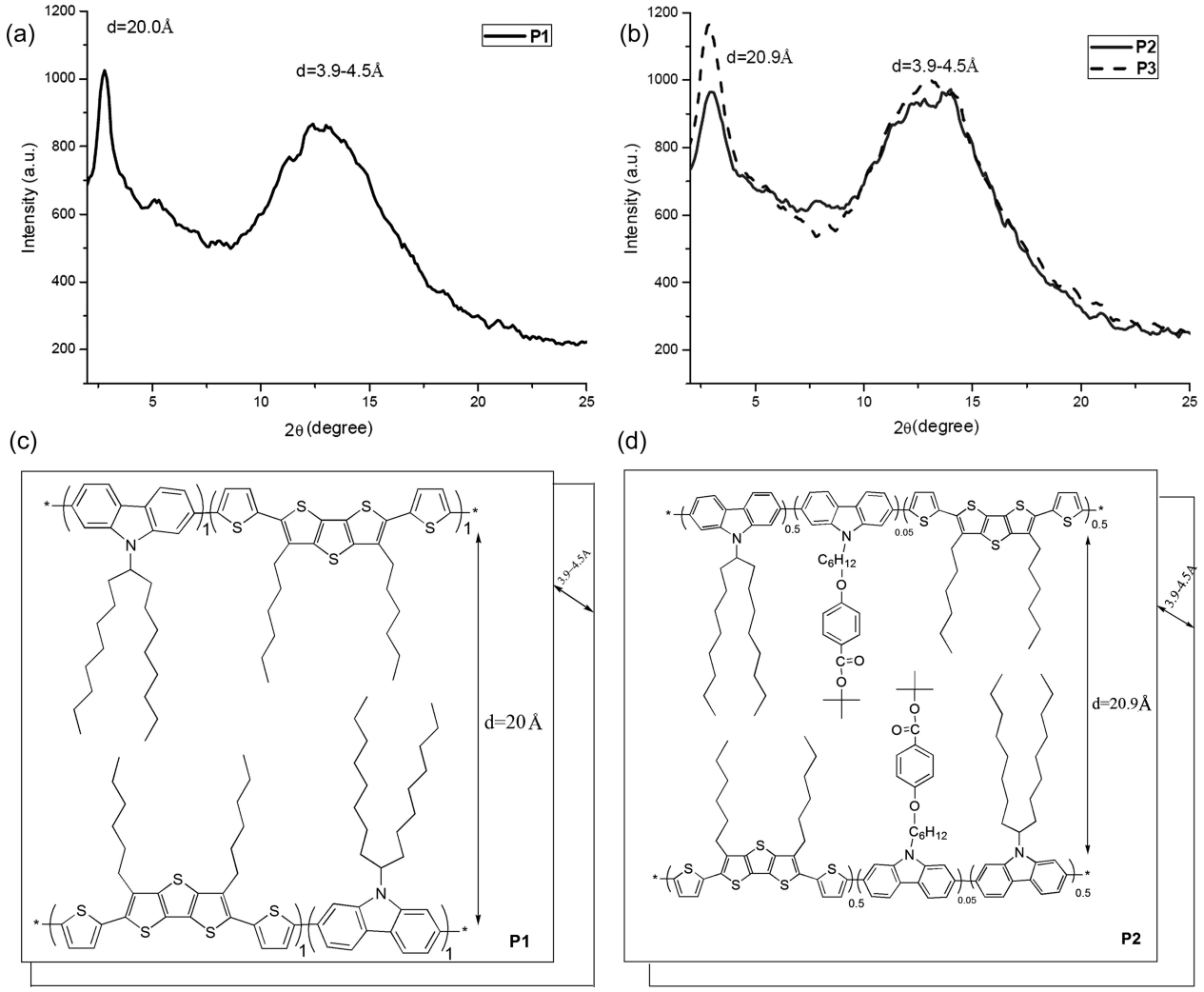

FIGURE 5 Powder X-ray diffraction (XRD) spectra of (a) **P1** and (b) **P2–P3**; and schematic representations of proposed three-dimensional layered and π-π stacked arrangements of (c) **P1** and (d) **P2** in their XRD measurements (**P3** is similar to **P2**).

temperature. **P1–P3** after thermal annealing exhibited substantially a primary diffraction feature with a angle at $2\theta = 2.9^\circ$ (corresponding to a large *d*-spacing value of 20 Å for **P1**) and $2\theta = 2.8^\circ$ (corresponding to a large *d*-spacing value of 21 Å for **P2–P3**), which were assigned to a distance between the conjugated backbones separated by the long side chains as reported for other similar π-conjugated polymers with long pendants.[25] Moreover, a much stronger (100) XRD characteristic peak of **P3** (with H-bonds) was observed in contrast to **P2** (without H-bonds). The XRD data demonstrate that **P3** possessed a larger crystallinity than **P2** which was enhanced by the H-bonded interactions. In our previous studies, the crystallinities of the supramolecular polymers were much improved due to the presence of hydrogen bonds, which enhanced the self-assembled behavior and thus to induce higher PCE values of H-bonded polymers.[26(a)] Moreover, the higher liquid crystalline arrangements of smectic layers can be induced by the formation of supramolecular structures with highly ordered H-bonds.[26(b,c)] The possible packing motifs of polymers **P1–P3** in the XRD measurements with three-dimensional layered and π-π stacked arrangements are represented in Figure 5(c,d), which show a model that the alkyl side chains stack as bilayered packings within the same layer. On the other hand, the reflections in the wide angle region (corresponding to 3.9–4.5Å) are related to the π-π stacked distance between the polymer layers,[27,28] which have the similar wide-angle *d*-spacing values and XRD intensities in all polymers **P1–P3** to show their almost fixed π-π stacking distances (ca. 3.9–4.5Å) with comparable crystallinities. The diffraction features of polymers **P1–P3** were often observed in the XRD patterns of the π-conjugated polymers.[29] Overall, the proposed model can explain the possible structural arrangements of the polymer chains in **P1–P3**, and the highest crystallinity of **P3** in the small and large angle regions of XRD pattern (corresponding to the bilayered packings between polymer backbones and the π-π stacked distance between the polymer layers, respectively) was induced by H-bonds.

Morphology

The AFM topographies of polymer blends (**P1–P3**: PCBM = 1:1 w/w) were investigated by the casting films of dichlorobenzene solutions as shown in Figure 6, where the images

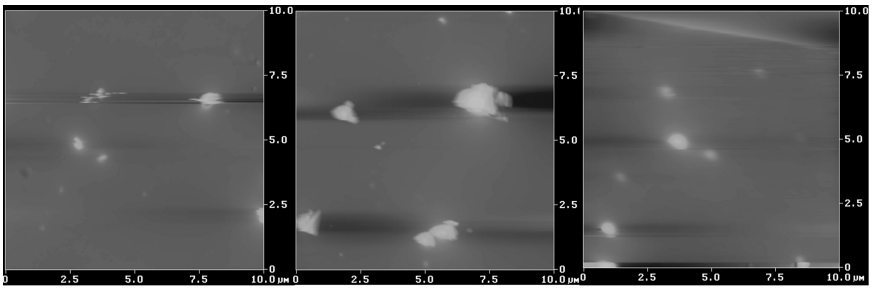

FIGURE 6 AFM images obtained from solid films of **P1–P3**/PCBM (1:1 w/w).

were obtained by the tapping mode. Furthermore, the solid films of blended copolymers **P1** and **P3** showed a similar surface roughness with moderate root mean square (RMS) values about 18 nm. In comparison with blended polymers **P1** and **P3**, blended polymer **P2** revealed a rather uneven surface with a RMS roughness of 58.6 nm, which was attributed to the aggregation of polymer chains due to their poor solubilities and lack of H-bonds, and thus to reduce the interface between donor (**P2**) and acceptor (PCBM) significantly. As shown in Table 3, owing to the unfavorable morphology for charge transport offered by poor solubility of **P2**, the PSC device based on **P2** gave relatively low current densities (I_{sc}) and thus the lowest PCE value. Therefore, the PCE values of blended polymers (**P1–P3**: PCBM = 1:1 w/w) are inversely proportional to their RMS roughnesses in AFM.

Photovoltaic Properties

The motivation for the design and syntheses of the conjugated polymers is to look for new polymers for the application of PSCs. To investigate the potential use of polymers **P1–P3** in PSCs, bulk heterojunction devices were fabricated from an active layer in which polymers **P1–P3** were blended with PCBM. PSC devices with a configuration of ITO/PEDOT: PSS/**P1–P3**: PCBM (w/w = 1:1)/Ca/Al were fabricated. The PSC devices were measured under simulated AM 1.5 solar illumination for a calibrated solar simulator with an intensity of 100 mW/cm^2. The preliminarily obtained properties are summarized in Table 3, and the typical *I–V* characteristics of all PSC devices are shown in Figure 7. Under monochromatic illumination, the power conversion efficiency (PCE) values of 0.44 to 0.61% were obtained for the PSC devices composed of polymers **P1–P3** with current density (J_{sc}), open circuit voltage (V_{oc}), and fill factor (FF) in the range of 2.02 to 2.27

TABLE 3 Photovoltaic Properties of PSC Devices Containing an Active Layer of Polymer: PCBM (1:1 w/w) with a Device Configuration of ITO/PEDOT: PSS/Polymer: PCBM/Ca/Al[a]

Active Layer (Polymer: PCBM = 1:1 w/w)	V_{oc} (V)	J_{sc} (mA/cm^2)	FF (%)	PCE (%)
P1	0.73	2.27	0.33	0.54
P2	0.71	2.02	0.31	0.44
P3	0.90	2.26	0.31	0.61

[a] Measured under AM 1.5 irradiation, 100 mW/cm^2.

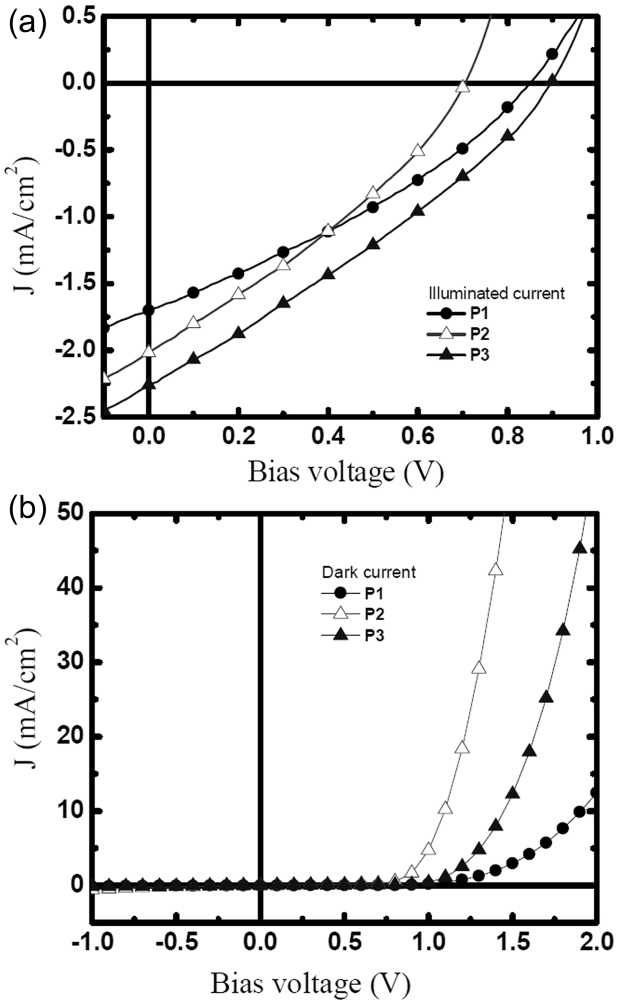

FIGURE 7 *I–V* curves (under simulated AM 1.5 solar irradiation) of solar cells with an active layer of **P1–P3**: PCBM measured by (a) illuminated current and (b) dark current.

mA/cm^2, 0.71 to 0.90 V, and 31 to 33%, respectively. The photovoltaic properties of the PSC devices containing fused dithienothiophene-based polymers **P1–P3** were dependent on the solubility and film-forming quality of the polymers. As mentioned in our introductory content, some donor polymers containing dithienothiophene units (designed and prepared by Millefiorini et al.,[12(b)] Gong et al.,[12(a)] and Zhang et al.[15(a)]) illustrated lower open circuit voltages ($\sim$ 0.8 V) and PCE values ($\sim$ 0.4%) than those of **P3**, even certain donor-acceptor copolymers[11(a),14] have worse photovoltaic properties than these developed polymers. Among these PSC devices containing **P1–P3** in Figure 7, polymer **P3** gave the best performance of PCE = 0.61% with J_{sc} = 2.26 mA/cm^2, V_{oc} = 0.90 V, and FF = 31%. The V_{oc} values are normally related to the HOMO energy levels of the polymers and the LUMO energy levels of the acceptors (e.g., PCBM).[30] Though the HOMO energy levels of **P1–P3** were similar, the V_{oc} value of **P3** was noticeably higher than those of **P1–P2**. Therefore, the highest PCE value of **P3** is associated with its highest V_{oc} value and highest crystallinity induced by H-bonds.

CONCLUSIONS

We have successfully synthesized three dithienothiophene/carbazole-based conjugated polymers (**P1–P3**) by Suzuki coupling reaction. Interestingly, **P1–P3** exhibited reversible electrochromism during the oxidation processes of cyclic voltammogram studies. Among **P1–P3**, polymer **P3** (with H-bonds) revealed the best electrochromic property with the most noticeable color change. In powder X-ray diffraction (XRD) measurements, these polymers exhibited obvious diffraction features indicating distinct bilayered packings between polymer backbones and similar π-π stacking between layers in the solid state. Compared with the XRD data of **P2** (without H-bands), H-bonds of **P3** induced a higher crystallinity in the small angle region (corresponding to a higher ordered bilayered packings between polymer backbones), but with a similar crystallinity in the wide angle region indicating a comparable π-π stacking distance between layers. The potential applications of **P1–P3** in bulk heterojunction photovoltaic solar cells (PSCs) were further investigated, where the PSC device containing **P3** blended with PCBM (by a weight ratio of 1:1) had the optimum power conversion efficiency (PCE) up to 0.61% (with J_{sc} = 2.26 mA/cm^2, FF = 29.8%, and V_{oc} = 0.90 V). Due to the H-bonded effects, polymer **P3** possessed higher thermal decomposition temperature (T_d), glass transition temperature (T_g), RMS smoothness, open circuit voltage (V_{oc}), and PCE value than **P2**. These polymers demonstrate a novel family of conjugated polymers along the path toward achieving the electrochromic and PSC applications.

ACKNOWLEDGMENTS

The financial supports of this project provided by the National Science Council of Taiwan (ROC) through NSC 99-2113-M-009-006-MY2, NSC 99-2221-E-009-008-MY2, and National Chiao Tung University through 97W807 are acknowledged. The powder XRD measurements are supported by beamline BL13A (charged by Ming-Tao Lee) of the National Synchrotron Radiation Research Center (NSRRC), in Taiwan.

REFERENCES AND NOTES

1 Yu, G.; Gao, J.; Hummelen, J. C.; Wudl, F.; Heeger, A. J. *Science* **1995,** *270*, 1789–1791.

2 Thompson, B. C.; Fréchet, J. M. J. *Angew. Chem. Int. Ed. Engl.* **2008,** *47*, 58–77.

3 Coffey, D. C.; Reid, O. G.; Rodovsky, D. B.; Bartholomew, G. P.; Ginger, D. S. *Nano Lett.* **2007,** *7*, 738–744.

4 (a) Moulé, A. J.; Meerholz, K. *Adv. Mater.* **2008,** *20*, 240–245; (b) Li, L.; Lu, G. H.; Yang, X. *J. Mater. Chem.* **2008,** *18*, 1984–1990; (c) Chang, Y. M.; Wang, L. *J. Phys. Chem. C* **2008,** *112*, 17716–17720; (d) Yao, Y.; Hou, J. H.; Xu, Z.; Li, G.; Yang,Y. *Adv. Funct. Mater.* **2008,** *18*, 1783–1789.

5 (a) Liang, Y.; Feng, D.; Wu, Y.; Tsai, S. T.; Li, G.; Ray, C.; Yu, L. *J. Am. Chem. Soc.* **2009,** *131*, 7792–7799; (b) Hou, J.; Chen, H. Y.; Zhang, S.; Chen, R. I.; Yang, Y.; Wu, Y.; Li, G. *J. Am. Chem. Soc.* **2009,** *131*, 15586–15587; (c) Park, S. H.; Roy, A.; Beaupré, S.; Cho, S.; Coates, N.; Moon, J. S.; Moses, D.; Leclerc, M.; Lee, K.; Heeger, A. J. *Nat. Photonics* **2009,** *3*, 297–302; (d) Liang, Y.; Xu, Z.; Xia, J.; Tsai, S. T.; Wu, Y.; Li, G.; Ray, C.; Yu, L. *Adv. Mater.* **2010,** *22*, 135–138; (e) Chen, H. Y.; Hou, J.; Zhang, S.; Liang, Y.; Yang, G.; Yang, Y.; Yu, L.; Wu, Y.; Li, G. *Nat. Photonics* **2009,** *3*, 649–653.

6 (a) Scharber, M. C.; Mühlbacher, D.; Koppe, M.; Denk, P.; Waldauf, C.; Heeger, A. J.; Brabec, C. J. *Adv. Mater.* **2006,** *18*, 789–794; (b) Günes, S.; Neugebauer, H.; Sariciftci, N. S. *Chem. Rev.* **2007,** *107*, 1324–1338.

7 (a) Lia, J.; Grimsdale, A. C. *Chem. Soc. Rev.* **2010,** *39*, 2399–2410; (b) Tamura, K.; Shiotsuki, M.; Kobayashi, N.; Masuda, T.; Sanda, F. *J. Polym. Sci. Part A: Polym. Chem.* **2009,** *47*, 3506–3517; (c) Blouin, N.; Michaud, A.; Leclerc, M. *Adv. Mater.* **2007,** *19*, 2295–2300.

8 (a) Leclerc, N.; Michaud, A.; Sirois, K.; Morin, J. F.; Leclerc, M. *Adv. Funct. Mater.* **2006,** *16*, 1694–1704; (b) Fu, Y.; Kim, J.; Siva, A.; Shin, W. S.; Moon, S. J.; Park, T. *J. Polym. Sci. Part A: Polym. Chem.* **2011,** *49*, 4368–4378.

9 (a) Blouin, N.; Michaud, A.; Gendron, D.; Wakim, S.; Blair, E.; Neaguplesu, R.; Belletete, M.; Durocher, G.; Tao, Y.; Leclerc, M. *J. Am. Chem. Soc.* **2008,** *130*, 732–742; (b) Zou, Y.; Gendron, D.; Aïch, R. B.; Najari, A.; Tao, Y.; Leclerc, M. *Macromolecules* **2009,** *42*, 2891–2894; (c) Qin, R. P.; Li, W. W.; Li, C. H.; Du, C.; Veit, C.; Schleiermacher, H. F.; Andersson, M.; Bo, Z. S.; Liu, Z. P.; Inganäs, O.; Wuerfel, U.; Zhang, F. L. *J. Am. Chem. Soc.* **2009,** *131*, 14612–14613; (d) Zhang, M.; Fan, H.; Guo, X.; He, Y.; Zhang, Z.; Min, J.; Zhang, J.; Zhao, G.; Zhan, X.; Li, Y. *Macromolecules* **2010,** *43*, 5706–5712.

10 (a) Ku, S. Y.; Liman, C. D.; Burke, D. J.; Treat, N. D.; Cochran, J. E.; Amir, E.; Perez, L. A.; Chabinyc, M. L.; Hawker, C. J. *Macromolecules* **2011,** *44*, 9533–9538; (b) Bae, W. J.; Scilla, C.; Duzhko, V. V.; Jo, W. H.; Coughlin, E. B. *J. Polym. Sci. Part A: Polym. Chem.* **2011,** *49*, 3260–3271.

11 (a) Zhang, S. M.; Guo,Y. L.; Fan, H. J.; Liu, Y.; Chen, H. Y.;Yang, G. W.; Zhan, X. W.; Liu, Y. Q.; Li, Y. F.; Yang, Y. *J. Polym. Sci. Part A: Polym. Chem.* **2009,** *47*, 5498–5508; (b) Li, K. C.; Hsu, Y. C.; Lin, J. T.; Yang, C. C.; Wei, K. H.; Lin, H. C. *J. Polym. Sci. Part A: Polym. Chem.* **2009,** *47*, 2073–2092; (c) Li, K. C.; Huang, J. H.; Hsu, Y. C.; Huang, P. J.; Chu, C. W.; Lin, J. T.; Ho, K. C.; Wei, K. H.; Lin, H. C. *Macromolecules* **2009,** *42*, 3681–3693.

12 (a) Gong, C.; Song, Q. L.; Yang, H. B.; Li, J.; Li, C. M. *Sol. Energy Mater. Sol. Cells* **2009,** *93*, 1928–1931; (b) Millefiorini, S.; Kozma, E.; Catellani, M.; Luzzati, S. *Thin Solid Films* **2008,** *516*, 7205–7208.

13 Zhan, X. W.; Tan, Z. A.; Domercq, B.; An, Z. S.; Zhang, X.; Barlow, S. *J. Am. Chem. Soc.* **2007,** *129*, 7246–7247; (b) Tan, Z. A.; Zhou, E. J.; Zhan, X. W.; Wang, X.; Li, Y. F.; Barlow, S. *Appl. Phys. Lett.* **2008,** *93*, 073309.

14 Huang, X. B.; Zhu, C. L.; Zhang, S. M.; Li, W. W.; Guo, Y. L.; Zhan, X. W. *Macromolecules* **2008,** *41*, 6895–6902.

15 (a) Zhang, S. M.; Fan, H. J.; Liu, Y.; Zhao, G. J.; Li, Q. K.; Li, Y. F.; Zhan, X. W. *J. Polym. Sci. Part A: Polym. Chem.* **2009,** *47*, 2843–2852; (b) Li, J.; Qin, F.; Li, C. M.; Bao, Q. L.; Chan-Park, M. B.; Zhang, W.; Qin, J. G.; Ong, B. S. *Chem. Mater.* **2008,** *20*, 2057–2059; (c) Kim, K. H.; Chung, D. S.; Park, C. E.; Choi, D. H. *J. Polym. Sci. Part A: Polym. Chem.* **2011,** *49*, 55–64.

16 (a) Würthner, F.; Chen, Z.; Hoeben, F. J. M.; Osswald, P.; You, C. C.; Jonkheijm, P. *J. Am. Chem. Soc.* **2004,** *126*, 10611–10618; (b) Hoeben, F. J. M.; Zhang, J.; Lee, C. C.; Pouderoijen, M. J.; Wolffs, M.; Würthner, F. *Chem. Eur. J.* **2008,** *14*, 8579–8589; (c) El-ghayoury, A.; Schenning, A. P. H. J.; Hal, P. A. V.; Duren, J. K. J. V.; Janssen, R. A. J.; Meijer, E. W. *Angew. Chem. Int. Ed. Engl.* **2001,** *40*, 3660–3663; (d) Jonkheijm, P.; Duren, J. K. J. V.; Kemerink, M.; Janssen, R. A. J.; Schenning, A. P. H. J.; Meijer, E. W. *Macromolecules* **2006,** *39*, 784–788.

17 He, M.; Zhang, F. *J. Org. Chem.* **2007,** *72*, 442–451.

18 Dennler, G.; Scharber, M. C.; Brabec, C. J. *Adv. Mater.* **2009,** *21*, 1323–1338.

19 (a) Wu, C. W.; Tsai, C. M. *Macromolecules* **2006,** *39*, 4298; (b) Wu, C. W.; Lin, H. C. *Macromolecules* **2006,** *39*, 7232–7240.

20 Coppo, P.; Cupertino, D. C.; Yeates, S. G.; Turner, M. L. *Macromolecules* **2003,** *36*, 2705–2711.

21 Brabec, C. J.; Sariciftci, N. S.; Hummelen. J. C. *Adv. Funct. Mater.* **2001,** *11*, 15–26.

22 Shahid, M.; Ashraf, R. S.; Klemm, E.; Sensfuss, S. *Macromolecules* **2006,** *39*, 7844–7853.

23 Al-Ibrahima, M.; Rotha, H. K.; Zhokhavetsb, U. *Sol. Energy Mater. Sol. Cells* **2005,** *85*, 13–25.

24 Mihailetchi, V. D.; Duren, J. K. J. V.; Blom, P. W. M.; Hummelen, J. C.; Janssen, R. A. J.; Kroon, J. M.; Rispens, M. T.; Verhees, W. J. H.; Wienk, M. M. *Adv. Funct. Mater.* **2003,** *13*, 43–46.

25 (a) Lu, G.; Usta, H.; Risko, C.; Wang, L.; Facchetti, A.; Ratner, M. A.; Marks, T. J. *J. Am. Chem. Soc.* **2008,** *130*, 7670–7685; (b) Yasuda, T.; Sakai, Y.; Aramaki, S.; Yamamoto, T. *Chem. Mater.* **2005,** *17*, 6060–6068; (c) Watanabe, K.; Osaka, I.; Yorozuya, S.; Akagi, K. *Chem. Mater.* **2012,** *24*, 1011–1024.

26 (a) Patra, D.; Ramesh, M.; Sahu, D.; Padhy, H.; Chu, C. W.; Wei, K. H.; Lin, H. C. *Polymer* **2012,** *53*, 1219–1228; (b) Liang, T. C.; Lin, H. C. *J. Polym. Sci. Part A: Polym. Chem.* **2009,** *47*, 2734–2753; (c) Liang, T. C.; Lin, H. C. *J. Mater. Chem.* **2009,** *19*, 4753–4763.

27 (a) Kokubo, H.; Sato, T.; Yamamoto, T. *Macromolecules* **2006,** *39*, 3959–396; (b) Yamamoto, T.; Arai, M.; Kokubo, H.; Sasaki, S. *Macromolecules* **2003,** *36*, 7986–7993.

28 Hou, Y.; Chen, Y.; Liu, Q.; Yang, M.; Wan, X.; Yin, S.; Yu, A. *Macromolecules* **2008,** *41*, 3114–3119.

29 (a) Zhang, M.; Tsao, H. N.; Pisula, W.; Yang, C.; Mishra, A. K.; Müllen, K. *J. Am. Chem. Soc.* **2007,** *129*, 3472–3473; (b) Cao, J.; Kampf, J. W.; Curtis, M. D. *Chem. Mater.* **2003,** *15*, 404–411; (c) Yamamoto, Y.; Lee, B. L. *Macromolecules* **2002,** *35*, 2993–2999; (d) Ong, B. S.; Wu, Y. L.; Liu, P.; Gardner, S. *J. Am. Chem. Soc.* **2004,** *126*, 3378–3379; (e) Morana, M.; Wegscheider, M.; Bonanni, A.; Kopidakis, N.; Shaheen, S.; Scharber, M.; Zhu, Z.; Waller, D.; Gaudiana, R.; Brabec, C. *Adv. Funct. Mater.* **2008,** *18*, 1757–1766.

30 Brabec, C. J.; Cravino, A.; Meissner, D.; Sariciftci, N. S.; Fromherz, T.; Rispens, M. T.; Sanchez, L.; Hummelen, J. C. *Adv. Funct. Mater.* **2001,** *11*, 374–380.